Designing a Novel Hybrid Material: Hydroxyl Iron (III) – Bentonite, Kaolinte Composites for Enhanced Phenol Removal from Wastewater: A Comparative Study

Egah G.O[1], Sha'Ato R[2], Ewenifa O.J[3], and Itodo A.U[4]

[1,3]Federal University Wukari, Taraba State, Nigeria

[2,4]Joseph Sarwuan Tarka University, Makurdi, Benue State, Nigeria

umarissac@gmail.com

Abstract

Phenol is a toxic pollutant in wastewater, regulated to ensure safe water sources. This study examines Hydroxyiron (III) bentonite (HBC) and kaolin (HKC) composites for phenol removal from aqueous solutions (5–25 mg/L). The composites, produced by mixing bentonite and kaolin with Hydroxyiron (III) in a 3:1 ratio and calcined at 600°C for 1 hour, were tested at pH 2-11 and 25°C, with adsorbent dosages from 0.5 to 2.5 g in 50 mL solutions. Adsorption thermodynamics were developed for 1 hour, and kinetics experiments were performed at 25°C with a range of 10-60 minutes. Adsorption capacity increased with time, temperature, and concentration. HBC and HKC had pH values of 7.20 and 7.37, pHzpc of 10.10 and 11.00, conductivities of 1.657 and 1.763 µS/cm, bulky densities of 1.214 and 1.185 g/cm³, and attrition rates of 27.21% and 27.91%, respectively. XRF, FTIR, and SEM analyses confirmed hydroxyl group presence, indicating hydrogen bonding with phenol. The Blanchard pseudo-second order model best described HBC ($R^2 = 0.906$), and the pseudo-first order model best described HKC ($R^2 = 0.957$). Data fit the Langmuir model, indicating monolayer adsorption. Positive enthalpy, entropy, and Gibbs free energy values showed endothermic and non-spontaneous

adsorption, with physisorption dominating chemisorption. Maximum adsorption efficiencies were 79.952% for HBC and 75.600% for HKC at 60 minutes, suggesting HBC is a more effective adsorbent. These results indicate that HBC and HKC can be used to remove organic pollutants from wastewater.

Keywords: Adsorption; Bentonite; Hydroxyiron (III); Kaolinite; Phenol

INTRODUCTION

The presence of phenol in wastewater has become a major source of concern to environmentalists because it is considered a toxic, hazardous and priority pollutant (Afaj *et al.,* 2015). Wastewaters discharged from pesticide, soap, paint, solvent, pharmaceuticals, paper and pulp industries, and also water disinfecting process constitute a major source of phenol (Girish and Murty, 2013). Phenol is water soluble and highly mobile and small amount may cause severe diseases like cancer, nausea, vomiting, paralysis, smoky colored urine (Afaj *et al.,* 2015). The maximum permitted concentration level of phenol according to US Environmental Protection Agency (EPA) is 0.5-1 mg/L for industrial wastewater and 1 μg/L for drinking water (Afaj *et al.,* 2015).

MATERIALS AND METHODS

Sampling and sample identification

The raw kaolin and bentonite used in this work were supplied from Somak Industries Nigeria Limited, Akoko-Edo L.G.A, Edo State and Knexel Nigeria Limited, no; 27, Adeleke Street, Ikeja, Lagos State, Nigeria respectively. The samples were taken for proper identification in the Department of Soil Science, Federal Universty Wukari, Taraba state.

Preparation of the adsorbents

Preparation of hydroxyiron (III)

Hydroxyiron (III) was prepared by reaction of an anhydrous ferric chloride $FeCl_3$ solution with sodium hydroxide NaOH solution which led to the formation of a precipitate. The precipitate was filtered using filter paper, dried in an oven for about 24 hrs and crushed

into powder. Finally, it was stored as $Fe(OH)_3$ in an air tight container for future use. The equation of reaction is shown in Equation (1);

$$FeCl_{3(aq)} + 3NaOH_{(aq)} \rightarrow Fe(OH)_{3(aq)} + 3NaCl_{(aq)} \qquad (1)$$
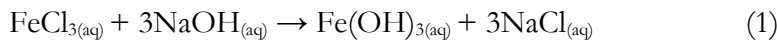
Preparation of hydroxyiron (III) (Fe(OH)₃) - bentonite composite (HBC) and hydroxyiron (III) (Fe(OH)₃) - kaolin composite (HKC).

The hydroxyiron (III) - bentonite composite (HBC) and hydroxyiron (III) - kaolin composite (HKC) were synthesized by combining raw bentonite and raw kaolin with hydroxyiron (III) (Fe(OH)₃) in a 3:1 ratio, followed by calcination at 600 °C for 1 hour. The resulting modified adsorbents, HBC and HKC, were then stored in a sealed container for future use (Syafalni *et al.,* 2013)

Physical characterization of adsorbents

The pH of the adsorbents was determined using a method described by Kibami *et al.,* (2014), while the point of zero charge (pHzpc) was determined by plotting the pH (final) vs pH (initial) curve. Conductivity was measured following the procedure outlined by Bansode (2002), and bulk density was determined using the tamping method described by Ahmedna *et al.,* (2000) as shown in Equation (2). These parameters provide important information about the physicochemical properties of the adsorbents.

$$\text{Bulk density (g/cm}^3) = \frac{\text{Mass of the adsorbent (g)}}{\text{Apparent Volume of adsorbent(cm}^3)} \qquad (2)$$

Attrition/Hardness (%)

The attrition or hardness of the adsorbents was determined using the wet attrition method described by Toles *et al.* (2000). This method measures the ability of the adsorbents to withstand mechanical stress during handling operations. The percentage of attrition was calculated based on the measured values as shown in Equation (3), providing insight into the durability of the adsorbents.

$$\text{Attrition (\%)} = \frac{\text{Initial mass(g)} - \text{Final mass(g)}}{\text{Initial mass(g)}} \times 100 \qquad (3)$$

Characterization of Adsorbents

The modified hydroxyiron (III) $(Fe(OH)_3)$ - bentonite composite (HBC) and hydroxyiron (III) $(Fe(OH)_3)$ - kaolin composite (HKC) chemical and mineralogical composition were characterized for by Fourier transformed infra-red (FTIR) for identification of surface functional groups, Scanning electron microscope (SEM) to determine the surface texture and porosity of the adsorbent and X-ray fluorescence (XRF) to determine the chemical composition of the adsorbents.

Batch Adsorption Experiment

Batch experiments were carried out according to methods adopted by Afaj *et al.,* (2015). In the batch adsorption experiment, 0.5 g of each adsorbent was contacted with 50 mL of known concentration adsorbate phenol solution in a conical flask (250 mL) in capacity, and stirred for (60 minutes) constant contact time by mechanical shaker at (200 rpm) at room temperature until equilibrium was achieved. At the end of the contact time required, the solution was filtered using filter paper and the filtrate analyzed for residual adsorbate concentrations for Phenol using UV-visible spectrophotometer at a maximum wavelength of 270 nm (Shimadzu, UV-1700 spectrophotometer).Batch adsorption experiments were performed by varying the pH, adsorbent dosage, concentration, contact time and temperature. Adsorption experiments on the amount of Phenol, Q_e (mg/g), was calculated by the mass balance equation (4) adopted by Kibami *et al.,* (2014)

$$Q_{e \, (mg/g)} = \frac{(C_o - C_e)}{M_a} V \qquad (4)$$

Where Q_e represent the adsorption capacity, C_o and C_e are the initial and residual Phenol concentrations (mg/L); V was the aliquot volume of phenol solution (L) used and m_a the mass of adsorbent in (g) used for a particular batch treatment. The percentage removal of phenol was calculated as shown in Equation (5):

$$\% \, Removal = \frac{(C_o - C_e)}{C_o} \times 100 \qquad (5)$$

% Removal is also called adsorption efficiency.

Adsorption Isotherms

The Langmuir and Freundlich adsorption isotherms models were applied in this research study.

Langmuir adsorption isotherm

The Langmuir model is based on assumptions of monolayer adsorption of adsorbate molecules on the adsorbent surface (Egah *et al.*, 2023). The Langmuir isotherm model is expressed as shown in equation (6):

$$\frac{1}{Q_e} = \frac{1}{Q_m} + \frac{1}{C_e} \times \frac{1}{bQ_m} \qquad (6)$$

Where Q_m (mg/g**)** is the monolayer sorption capacity for the adsorbate-adsorbent, representing the total binding sites available for sorption, C_e is the solute concentration in the bulk solution (mg/L), Q_e (mg/g) is the amount of solute sorbed by the adsorbent per unit mass and b (L/mg) is the Langmuir constant for the Adsorbate-Adsorbent. The higher the magnitude of b, the stronger the bond formed (Chen, 2015). The langmuir separation factor, R_L is expressed as;

$$R_L = \frac{1}{(1+bc_0)} \qquad (7)$$

If $R_L > 1$, is unfavourable, $R_L = 1$ is linear, R_L between 0 - 1 is favourable and $R_L = 0$ is irreversible (Egah *et al.*, 2019).

Freundlich adsorption isotherm

The Freundlich adsorption isotherm is based on multilayer adsorption on the heterogeneous surface of adsorbent containing different amount of energies (Bansal and Goyal, 2005). The linear equation as adopted by Krishna and Swamy, (2012) is given as:

$$logQ_e = \frac{1}{n_f}logc_e + logK_f \qquad (8)$$

Where Q_e (mg/g) is the amount adsorbed per unit mass of the adsorbent and C_e (mg/L) is the equilibrium concentration. K_f is the Freundlich isotherm constants representing the adsorption capacity and n_f is the adsorption intensity (Bansal and Goyal, 2005). If n values are between 1 to 10, they are classified as good adsorption according to Freundlich as reported by Krishna and Swamy, (2012).

Kinetics of Adsorption

The kinetic data were tested with pseudo-first-order and pseudo-second-order model as adopted by Essomba *et al.,* (2014).

Pseudo first order model

The Lagergren first-order equation as adopted by El-Dars *et al.,* (2016) is as expresses as

$$\log(Q_e - Q_t) = \log Q_e - \frac{K_1}{2.303}t \qquad (9)$$

Where Q_t is the amount of adsorbate adsorbed per unit mass of the adsorbent (mg/g) at time t (min). Q_e is the amount of adsorbate adsorbed per unit mass of the adsorbent in (mg/g), k_1 is the pseudo first order rate constant (L/min) (El-Dars et al., 2016).

Blanchard pseudo-second order model

Pseudo second order was presented by Egah *et al.,* (2019) as:

$$\frac{t}{Q_1} = \frac{1}{K_2 Q_{e^2}} + \frac{1}{Q_e}t \qquad (10)$$

Where K_2 is the pseudo-second order rate constant (g.mg^{-1}.min$^{-1)}$) and the initial adsorption rate, h (mg/g.min) = $K_2 Q_e^2$.

Thermodynamics Studies

The adsorption thermodynamics were applied to obtain the free energy change ΔG^0 in (kJmol^{-1}), enthalpy change ΔH^0 in (kJmol^{-1}) and the entropy change ΔS^0 in (JK^{-1}mol^{-1}). The thermodynamics equation given as:

$$\log\left(\frac{q_e}{C_e}\right) = \frac{\Delta S°}{2.303R} - \left(\frac{\Delta H°}{2.303R}\right)\frac{1}{T} \qquad (11)$$

Where Q_e/C_e is the adsorption affinity, R is the universal gas constant (8.314 Jmol^{-1}K^{-1}), T is the temperature in (K). The free Gibbs energy is given as calculated as:

$$\Delta G° = \Delta H° - T\Delta S° \qquad (12)$$

Where T is the standard temperature (298 K)

RESULTS AND DISCUSSION

Physicochemical Attribute of the Adsorbents

The physicochemical attributes of HBC and HKC adsorbents were evaluated as illustrated in Table 1. The pH values for HBC and HKC were close to neutral, indicating their neutral nature. The pH at point of zero charge (pHzpc) for both adsorbents was above 7.0, indicating a positively charged surface. The conductivity of HBC and HKC was low (2 μS/cm), suggesting good conductivity for the adsorption process. The bulk density of HBC and HKC was above 1 g/cm3, indicating favorable densities for adsorption. The percentage attrition for HBC and HKC was low (27.21% and 27.91%), indicating minimal abrasion losses during utilization compared to acid-activated almond shell based carbon. Overall, these findings suggest that both adsorbents possess favorable physicochemical attributes for adsorption Bansode, (2002).

**Table 1: Selected Physicochemical Attributes of Adsorbents**

Attribute	HBC	HKC
Ph	7.20	7.37
Conductivity (2μS/cm)	1.657	1.763
Bulk-density (g/cm^3)	1.214	1.185
Attrition (%)	27.21	27.91

FTIR Analysis of Adsorbents

The FTIR analysis is as shown in Figures 1. The FTIR spectrum of HBC exhibited similar characteristics. The broad band in the range of 3000-4000 cm^{-1} was associated with -OH group stretch from alcohol coordinated to octahedral Al^{3+} cations and water molecules adsorbed on the alumina octahedral layers and internal hydroxyl groups. This suggested that adsorption may have occurred on the -OH bending of water and the Si-O bond linkage in the hydroxyiron (III)-bentonite composite. In the FTIR spectrum of HKC, the bands at 3694.46 cm^{-1} were attributed to -OH groups from alcohol at the surface of the alumina octahedral layers interacting with the adjacent silica tetrahedral layers (Al-O-H). The band at 3627.46 cm^{-1} represented internal hydroxyl groups. The bands at 3466.00 cm^{-1} were associated with the bending vibrations of free water molecules adsorbed to the surface of hydroxyiron (III)-kaolin composites, indicating absorption at the outer surface (hygroscopic moisture) of the composites. In comparison with Kibami *et al.,* (2014), these

findings indicate the presence of relevant functional groups on the adsorbents, which are important for their adsorption properties and potential for phenol removal.
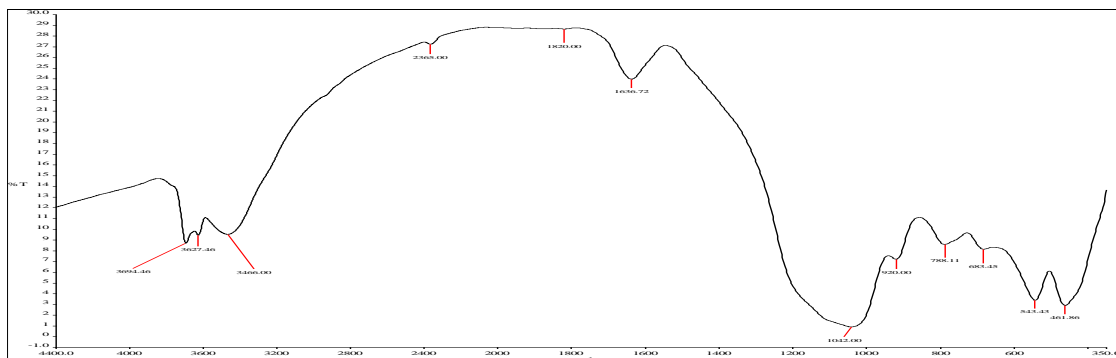
(a)
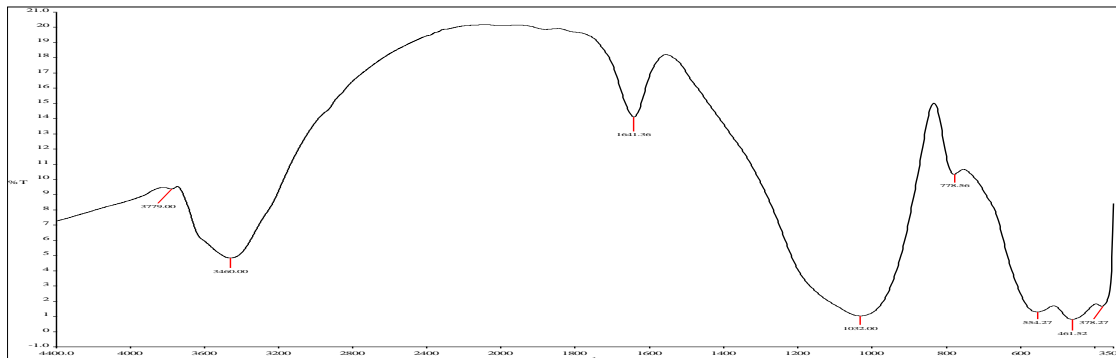
(b)

Figure 1: FTIR Spectrum of Hydroxyiron (III) - Bentonite Composite (HBC) (a) and Hydroxyiron (III) - Kaolin Composite (HKC)(b)

XRF Characterization of Adsorbents

XRF analysis as shown in Table 2 was conducted to determine the chemical composition of hydroxyiron (III) - bentonite and hydroxyiron (III) - kaolin composites. The results revealed a reduction in SiO_2 and Al_2O_3 percentages, possibly due to impurity decomposition during calcination. Conversely, an increase in SO_3 and Fe_2O_3 percentages suggested the addition of hydroxyiron (III) to the composites. Similar observations were reported in previous studies by Syafalni *et al*., (2013). The XRF analysis of hydroxyiron (III) - kaolin composite also showed a reduction in percentage weight, indicating impurity decomposition during calcination, along with an increase in SO_3 and Fe_2O_3 percentages

from hydroxyiron (III) addition. Additionally, complete decomposition of TiO_2 and MnO was observed, indicating their absence in the composite.

Table 2: X- Ray Fluorescence Chemical Characterization of the Adsorbents

OXIDE	HBC (wt %)	HKC (wt%)
Al_2O_3	13.0992	20.5065
SiO_2	32.9828	22.4080
P_2O_5	1.1369	1.7043
SO_3	21.3949	42.1455
K_2O	1.6250	0.3052
CaO	0.1420	0.3878
Fe_2O_3	28.1288	9.5985
ZnO	0.1026	0.1495
SnO_2	0.7168	1.4298
Sb_2O_3	0.6271	1.3650
TOTAL	100.00	100.00

Scanning Electron Microscopy of Adsorbents

SEM analysis was performed to examine the surface morphology of the adsorbents. The micrographs of hydroxyiron (III) bentonite composite (HBC) and hydroxyiron (III) kaolin composite (HKC) as shown in Plate 1 and 2 showed distinct features. HBC exhibited a porous, rough, and irregular surface with a crystalline structure, indicating the presence of macro-pores favorable for adsorption. This aligns with previous findings and suggests that HBC offers a higher adsorption capacity due to its external surface characteristics. In contrast, HKC displayed a compact structure with tubular crystals and uniform particle size, indicating an increased number of surface active sites for adsorption. This enhancement in adsorption capacity is consistent with similar observations reported by Moradi *et al.,* (2015). Overall, the SEM results indicate that both HBC and HKC possess favorable surface properties for effective adsorption
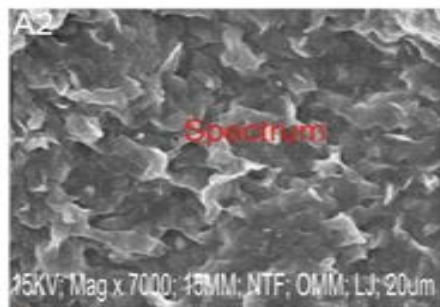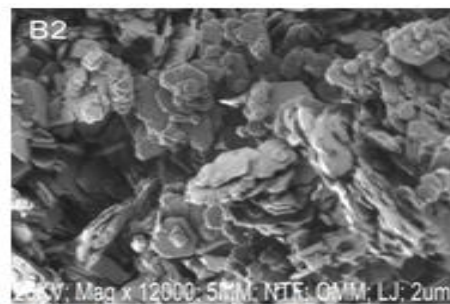
Plate1: Scanning Electron Microscope (SEM) of HBC

Plate 2: Scanning Electron Microscope (SEM) of HKC

The Adsorption of Aqueous Phenol Solution

Results of the batch experiments are shown on Figures 2a-c. The pH of the solution significantly influenced the adsorption of phenol, with the highest removal observed at pH 7 due to increased electrostatic attraction between the adsorbate and adsorbents (Ahmed *et al.,* 2015). Increasing the dosage of HBC and HKC adsorbents resulted in higher phenol removal percentages, indicating enhanced sorbent-solute interactions (Bhattacharyya and Gupta, 2011). Additionally, the adsorption of phenol increased with increase in contact time, while higher temperatures positively impacted phenol removal through enhanced oxidation or ionization.
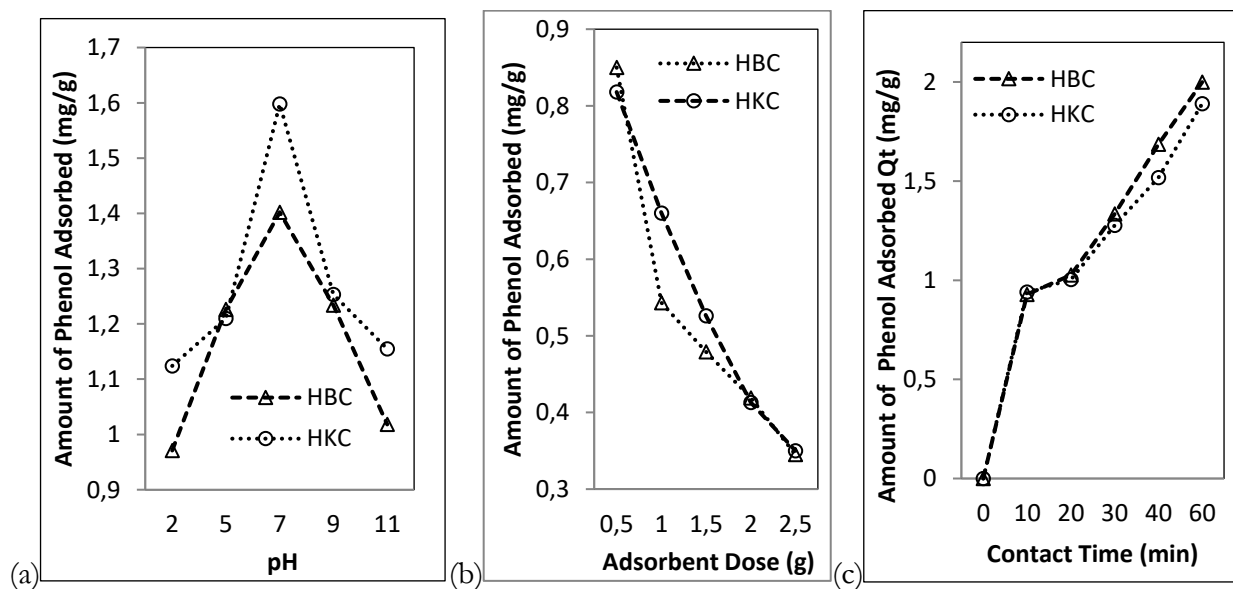

Figure 2: Effect of Initial Solution pH, Adsorbent Dosage and Contact Time on Aqueous Phase Adsorption of Phenol.

Adsorption Kinetics

Rate curve for adsorption of phenol

The rate curve analysis indicated that the adsorption capacity increased continuously from 10 to 60 minutes. The initial 10 minutes showed a rapid adsorption rate, suggesting an abundance of available adsorption sites compared to the initial bare surface density of the adsorbent (Ahmed *et al.,* 2015). At 60 minutes, the highest adsorption capacities of 1.999 mg/g for HBC and 1.890 mg/g for HKC were observed for phenol. This observation can be attributed to the saturation of active sites on the adsorbent as the adsorbed ions occupied these sites over time. This finding aligns with previous research by Bhattacharyya and Gupta (2011) and Ahmed *et al.,* (2015) on the removal of metal ions using clay-based adsorbents.

Adsorption kinetic model

Results in Table 3 show the kinetics parameters of phenol adsorption. The kinetic analysis of phenol adsorption on HBC and HKC revealed that both the first-order and pseudo-second-order models could describe the adsorption process. The Blanchard pseudo-second-order model best described the adsorption of phenol on HBC, while the pseudo-first-order model was more suitable for HKC. The adsorption capacities increased with contact time, indicating a predominant physisorption process.

Table 3: Kinetic Parameter for Adsorption Lagergren First Order and Blanchard Second Order for Phenol.

Adsorbate	Model	Adsorbents	
Phenol	**First order**	**HBC**	**HKC**
	K_1 (Lmin^{-1})	0.041	0.035
	Q_e (mg/g)	1.886	1.626
	R^2	0.885	0.957
Phenol	Second order		
	K_2 (g.mg^{-1}min^{-1})	0.012	0.016
	Q_e (mg/g)	2.878	2.537
	R^2	0.906	0.916
	h (gmg^{-1}min^{-1})	0.099	0.102

Adsorption Isotherms Studies

Langmuir and Freundlich adsorption isotherm models were used to analyze the equilibrium data according to Table 4. The Langmuir indicates regression coefficients R^2 values of (0.961 and 0.984) and Freundlich (0.951 and 0.970) for HBC and HKC respectively. Data fitted the Langmuir isotherm with higher R^2 values than Freundlich isotherm, indicating a monolayer adsorption (Egah *et al.,* 2023). From the results in Table 5, the Langmuir model yielded maximum adsorption capacities (Q_m) of 6.042 mg/g for HBC and 7.047 mg/g for HKC, representing the number of binding sites for adsorption phenol. From the results, HKC has the ability to adsorb more phenol than HBC. The Langmuir factor b (L/mg) which determines the interaction between adsorbent and adsorbate were found to be 0.032 and 0.022 L/mg for HBC and HKC respectively. According to Egah *et al.,* (2019), b>0, b<0, and b=0 indicates favorable, unfavorable and no interaction respectively. Since b>0, it means that adsorption is favorable. The Langmuir constant R_L, which measures strength of interaction between adsorbate and adsorbent specific sites are given as 0.862 and 0.901 for HBC and HKC. Also, R_L>0, R_L<0, and R_L= 0 represents favorable, unfavorable and no interaction respectively. The Freundlich adsorption capacity K_F ((mg/g)L/mg)1/n) relates to concentration of solute and it adsorption on solid surface. The K_F values were found to be (0.139 and 0.141 mg/g) for HBC and HKC, representing strong adsorbents-adsorbate interaction due high surface area (Sha'Ato *et al.,* 2018). The n_F values were found to be 1.000 and 1.011 for HBC and HKC indicating linear and favorable adsorption respectively.

Table 4: Isotherm Parameters for Phenol Adsorption on Adsorbents

Adsorbate	Model	Adsorbent	
Phenol	**Langmuir**	**HBC**	**HKC**
	Q_m(mg/g)	6.042	7.047
	b (L/mg)	0.032	0.022
	R^2	0.961	0.984
	R_L	0.862	0.901
Phenol	**Freundlich**		
	1/n	1.011	0.990
	n_F	1.000	1.011
	R^2	0.951	0.970
	K_F((mg/g) L/mg)1/n)	0.139	0.141

Thermodynamic Parameter for Adsorption of Phenol

Thermodynamics plays a crucial role in determining the spontaneity of adsorption processes. Table 5 shows that both HBC and HKC exhibited high values for endothermic reactions with ΔH values of 40.378kJ/mol and 29.766kJ/mol for HBC and HKC. As indicated from Table 5, the value of $\Delta H°$ for HBC and HKC are within the values of 20 - 40 kJ/mol, indicating physical adsorption (Allam *et al.,* 2018). The positive values of ΔS^0 (115.455 J/molK for HBC and 80.179 J/molK for HKC) indicate a high degree of disorder at the solid-liquid interface during adsorption (Nethaji *et al.,* 2013). The positive values of ΔG^0 (2.508 kJ/mol for HBC and 3.468 kJ/mol for HKC) suggest that the adsorption reactions are non-spontaneous and activation (Allam *et al.,* 2018).

Table 5: Thermodynamic Parameters of Adsorption for Phenol

Adsorbate	Adsorbens	ΔH(kJ/mol.1000)	ΔS(J/molK)	R^2	ΔG(kJ/mol.1000)
Phenol					
	HBC	40.378	115.455	0.994	2.508
	HKC	29.766	80.179	0.986	3.468

CONCLUSION

Hydroxyiron (III) - Bentonite Composite (HBC) and Hydroxyiron (III) - Kaolin Composite (HKC) were tested to eliminate the phenol from aqueous solution. The investigation has allowed the comparison of their adsorption capacity. The optimum pH for the adsorption of phenol was found to be pH 7. The adsorption of phenol increases with increase initial concentration. Adsorptions data were best described by the Langmuir model indicating monolayer adsorption. For the kinetic studies the pseudo second order best described HBC, while pseudo first order best described HKC. From the thermodynamics result the $\Delta H°$ for HBC and HKC are within the values of 20 - 40 kJ/mol, indicating physical adsorption. The positive values of ΔG indicate the requirement of activation energy. From the overall results Hydroxyiron (III) - Bentonite Composite (HBC) and Hydroxyiron (III) - Kaolin Composite (HKC could be used to remove organic pollutants from wastewater.

REFERENCES

Afaj, H. A., Mohammad, R. M., and Mahmoud N. M. (2015). Removal of phenol from Industrial Effluents using Activated Carbon and Iraqi Porcelanite Rocks – A Comparative Study. *Journal of Ministry of Science and Technology. 91*: 21-32.

Ahmed, A. S., Tantawy, A. M., Abdallah, M. E. and Qassim, I. M. (2015). Characterization and application of kaolinite clay as solid phase extractor for removal of copper ions from environmental water samples. *International Journal of Advanced Research. 3*(3): 1-21.

Ahmedna, M., Marshall, W. E and Rao, R. M. (2000). Production of granular activated carbon from select agricultural by-products and evaluation of their physical, chemical, and adsorptive properties. *Bio-resource Technology. 71*(2): 113-123.

Allam, K., Gourai, K. E. L., Bouari, A., Belhorma, B., & Bih L. (2018).Adsorption of Methylene Blue on raw and activated Clay: case study of Bengurir clay. *Journal of Materials and Environmental Sciences, 9*(6): 1750-1761 https://doi.org/10.26872/jmes.2018.9.6.195.

Bansal, R. C. & Goyal, M. (2005). Activated carbon adsorption. *Journal water resource and protection, 6*(9): 145-196. http://dx.doi.org/10.1201/9781420028812.

Bansode, R.R. (2002). "Treatment of Organic and Inorganic Pollutants in Municipal Wastewater by Agricultural by-product based Granular Activated Carbon (GAC)". Unpublished M.Sc. thesis. Louisiana State University and Agricultural and Mechanical College. Pp96.

Bhattacharyya, K. G., & Gupta, S.S. (2011). Removal of Cu (II) by natural and acid-activated clays: an insight of adsorption isotherm, kinetics and thermodynamics. *Desalination, 272*: 66–75.

Chen, X. (2015). Modeling of Experimental Adsorption Isotherm Data. *Open access Information journal, 6*:14-22. DOI:10.3390/info6010014

Egah, G. O., Hikon, B. N., Ngantem, G. S, Yerima, E. A., Omovo, M., Ogah E and Aminu, F. A. (2019). Synergistic Study of Hydroxyiron (III) and Kaolinite Composite for the Adsorptive Removal of Phenol and Cadmium. *International Journal of Environmental Chemistry. 3*(1): 30-42. doi: 10.11648/j.ijec.20190301.15

Egah, G. O., Sha''Ato, R., Itodo, A. U. & Wuana, R. A. (2023). Sorption of tartrazine dye from aqueous solution using activated carbon prepared from Cocos nucifera husk, *International Journal of Scientific Research Updates, 06*(01): 093–106 DOI: https://doi.org/10.53430/ijsru.2023.6.1.0061

El-Dars, E. S. M. F., Ibrahim, M. H., Farag, B. A. H., Abdelwahhab, Z. M and Shalabi, H. E. M. (2016). Preparation, Characterization of Bentonite Carbon Composite And Design Application In Adsorption Of Bromothymol Blue Dye. *Journal of Multidisciplinary Engineering Science and Technology, 3*(1): 3758-3765.

Essomba, S. J., Ndi Nsami, J., Belibi Belibi, B. P., Tagne, M. G. and Ketcha Mbadcam, J. (2014). Adsorption of Cadmium(II) Ions from Aqueous Solution onto Kaolinite and Metakaolinite. *Journal, Pure and Applied Chemical Sciences, 2*(1): 11 – 30

Krishna, H. R. and Swamy, S. V. V. A. (2012). Physico-Chemical Key Parameters, Langmuir and Freundlich isotherm and Lagergren Rate Constant Studies on the removal of divalent nickel from the aqueous solutions onto powder of calcined brick. *International Journal of Engineering Research and Development, 4*(1):29-38

Kibami, D., Pongener, C., K. S. Rao, K.S. and Sinha, D. (2014). Preparation and characterization of activated carbon from Fagopyrum esculentum Moench by HNO_3 and H_3PO_4 chemical activation. *Der Chemica Sinica. 5*(4):46-55

Moradi, M., Dehpahlavan, A., Kalantary, R. R., Ameri, A., Farzadkia, M. and Izanloo, H. (2015). Application of modified bentonite using sulfuric acid for the removal of hexavalent chromium from aqueous solutions. *Environmental Health Engineering and Management Journal, 2*(3): 99–106

Nethaji, S., Sivasamy, A. & Mandal, A. B. (2013). Adsorption isotherms, kinetics and mechanism for the adsorption of cationic and anionic dyes onto carbonaceous particles prepared from Juglans regia shell biomass, *International Journal of Environmental Science and Technology, 10*:231–242. DOI 10.1007/s13762-012-0112-0

Sha˝Ato, R., Egah, G.O. and Itodo, A.U. (2018). Aqueous phase abatement of phenol and cadmium using Hydroxyiron (III) calcined with bentonite. *Fuw Trends in Science and Technology Journal, 3*(1): 1 – 10.

Syafalni, Abdullah, R., Abustan, I. and Ibrahim, M. N.A . (2013). Wastewater treatment using bentonite, the combinations of bentonite-zeolite, bentonite-alum, and bentonite- limestone as adsorbent and coagulant. *International Journal of Environmental Sciences, 4*(3):379-391

Toles, C. A., Marshall, W. E., Johns, M. M., Wartelle, L. A. and McAloon, A. (2000). Acid Activated carbons from almond shells: physical, chemical and adsorptive properties and estimated cost of production. *Journal Bioresource Technology, 71*:87-92.